A miniaturized alpha spectrometer for the calibration of an avalanche-confinement TEPC

D. Bortot [a, b, *], A. Pola [a, b], S. Agosteo [a, b], S. Pasquato [a], M.V. Introini [a], P. Colautti [c], V. Conte [c]

[a] Politecnico di Milano, Dipartimento di Energia, Via La Masa 34, Milano, Italy
[b] Istituto Nazionale di Fisica Nucleare INFN, Sezione di Milano, Via Celoria 16, Milano, Italy
[c] Istituto Nazionale di Fisica Nucleare INFN, Laboratori di Legnaro, Viale Dell'Università 2, Legnaro (Padova), Italy

HIGHLIGHTS

- Selection of a miniaturized SSD for energy calibration of an innovative TEPC.
- A compact and removable Cm-244 alpha source embedded in the TEPC sensitive volume.
- Coincidence technique with the SSD signal to define the alpha particles path.
- Assessment of TEPC calibration factors for different simulated sites and voltages.

ARTICLE INFO

Keywords:
Microdosimetry
Tissue equivalent proportional counter (TEPC)
TEPC calibration
Solid state detector (SSD)
Cm-244 alpha source

ABSTRACT

The design and development of a recent avalanche-confinement tissue equivalent proportional counter (TEPC) for microdosimetry and nanodosimetry applications required the selection of a proper miniaturized solid state detector (SSD) for detecting alpha particles emitted by a thick removable Cm-244 source embedded in the cylindrical TEPC chamber for characterization and calibration purposes. Since the available cavity for embedding the SSD detector is only 4.2 mm in diameter, no standard devices can be exploited. The selection of the best SSD for this application was based on the following requirements: very low size, proper energy resolution, cheapness. The performances of the finally selected SSD were assessed by exploiting a multi-peak calibration alpha source (Pu-239, Am-241, Cm-244). The measured energy resolution resulted about 25 keV FWHM. The TEPC calibration procedure, which exploits the selected SSD aligned to the built-in Cm-244 alpha source, is described in details.

1. Introduction

The tissue equivalent proportional counter (TEPC) is the most accurate device for measuring the microdosimetric properties of a particle beam, showing to assess the relative biological effectiveness by linking the physical parameters of the radiation with the corresponding biological response (Wambersie et al., 2006). Nevertheless, no detailed information on the track structure of the impinging particles can be obtained, since the lower operation limit of the common TEPCs is about 0.3 μm (Hogeweg, 1973). On the other hand, the pattern of particle interactions at the nanometer level is measured by track-nanodosimetry, which assesses the single-event distribution of ionization cluster size for site dimensions from a few nanometers up to tens of nanometers. Anyway, only three detectors are available worldwide (De Nardo et al., 2002; Garty et al., 2002; Pszona and Gajewski, 1994).

In order to fill the gap between standard TEPCs and nanodosimeters, a feasibility study of a novel TEPC designed to simulate tissue equivalent sites in the nanometric domain was performed. In particular, an innovative avalanche-confinement TEPC based on a three-electrode structure and capable of performing microdosimetric measurements from 0.3 μm down to 25 nm in simulated site size, was designed basing on a prototype described elsewhere (Cesari et al., 2002).

TEPCs measure the pulse height spectra due to charged particles

* Corresponding author. Politecnico di Milano, Dipartimento di Energia, via La Masa 34, Milano, Italy.
E-mail address: davide.bortot@polimi.it (D. Bortot).

ionizing the tissue equivalent gas. The raw pulse height spectra are calibrated in terms of lineal energy with calibration functions. Most commercial TEPCs are equipped with a built-in alpha particle source, as Cm-244 or Am-241, for calibration. However, this procedure is generally affected by several uncertainties, mainly the discrepancy between the nominal energy of the alpha particle given by the manufacturer and the effective energy and the unknown details of the geometrical path of alpha particles within the sensitive volume (Schrewe et al., 1988). In order to overcome these limitations, the design of the new TEPC accounted for a removable internal Cm-244 source and a very compact solid state detector (SSD) inserted inside the sensitive zone (Fig. 1): this configuration allows calibrating the TEPC by also varying i) the simulated site size and ii) the polarization of the three electrodes. Moreover, only alpha particles crossing the sensitive volume parallelly to the anode wire are selected by the coincidence technique with the SSD signal, thus defining their path accurately.

Since the cavity for embedding the SSD detector has a really small size (4.2 mm in diameter), no standard devices can be exploited and different possible solutions were considered. The selection of the best device for this application was based on the following requirements: very low size, proper energy resolution and cheapness.

2. Selection of the solid state detector

Different commercial photodiodes with small external cases (type TO-18 or similar) were considered as possible candidates for the cited application: three devices of the Photonic Detectors, models PDU-C103, PDU-V103 and PDB-C136F, the API SD 057-11-21-011, the Pacific Silicon Sensor PC2-6-TO52-S1, the Marktech MTPD1346-150, the Hamamatsu S5972 and the Osram BPX65. They show different sensitive areas, both in size and shape (circular or square), different performances (in terms of energy resolution, junction capacitance and dark current) and different costs.

Among these devices, the silicon photodiodes Hamamatsu S5972 and Osram BPX65 were selected because of their good characteristics and low cost.

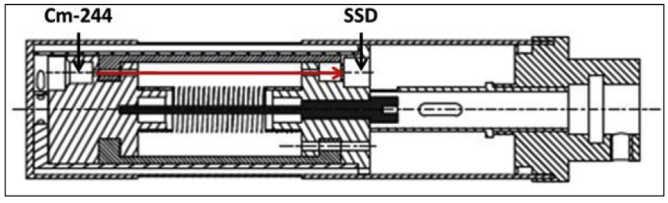

Fig. 1. Geometrical configuration adopted for characterization and calibration of the avalanche-confinement TEPC: this set-up allows selecting, by the coincidence technique with the SSD signal, only alpha particles emitted by the Cm-244 source crossing the sensitive volume parallelly to the anode wire, thus defining their path accurately (red arrow). (For interpretation of the references to colour in this figure legend, the reader is referred to the web version of this article.)

2.1. Hamamatsu S5972

The Hamamatsu S5972 (Hamamatsu website) is a high-speed silicon PIN photodiode designed for visible to near infrared light detection. This photodiode provides wideband characteristics at a low bias, making it suitable for optical communications and other high-speed photometry. It has a photosensitive circular area equal to 0.5 mm^2 embedded in a TO-18 package (Fig. 2). It shows a junction capacitance of 3 pF at 10 V of reverse bias voltage. Its main characteristics are listed in Table 1.

2.2. Osram BPX65

The Osram BPX65 (Osram website) is a high-speed silicon PIN photodiode with a sensitive area equal to 1×1 mm^2 embedded in a TO-18 package (Fig. 2). It shows a junction capacitance of about 3 pF at 10 V of reverse bias voltage. Its main characteristics are listed in Table 1. Its sensitive area is greater than the area of the Hamamatsu S5972 (greater detection efficiency) but the typical dark current results higher.

2.3. Experimental set-up

The performances of the two selected solid state detectors were experimentally assessed by exploiting a multi-peak calibration alpha source (Pu-239, Am-241, Cm-244) 3×10^3 Bq in nominal activity: Table 2 lists the energies and the relative intensities of the emitted alpha particles (National Nuclear Data Center, NuDat 2.6). The alpha source and each photodiode were placed inside a vacuum

Table 1
Hamamatsu S5972 and Osram BPX65 photodiodes: main characteristics (Hamamatsu and Osram websites).

	Hamamatsu S5972	Osram BPX65
Package	TO-18	TO-18
Active area	0.5 mm^2	1×1 mm^2
Maximum reverse voltage	20 V	20 V
Spectral response range	320–1000 nm	350–1100 nm
Typical dark current	0.01 nA (@ 10 V)	0.4 nA (@ 10 V)
Maximum dark current	0.5 nA (@ 10 V)	5 nA (@ 20 V)
Junction capacitance	3 pF (@ 10 V)	3 pF (@ 10 V)

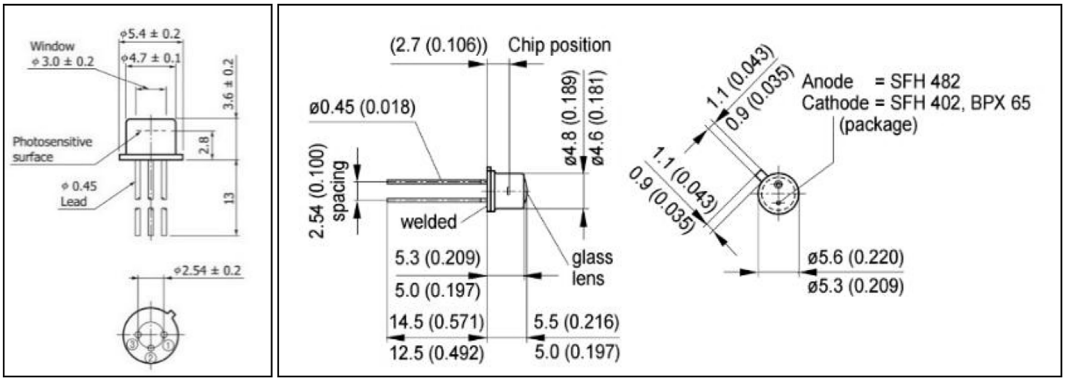

Fig. 2. Hamamatsu S5972 (left) and Osram BPX65 (right) photodiodes: dimensional outlines, in mm (Hamamatsu and Osram websites).

Table 2
Energies and relative intensities of the alpha particles emitted by the multi-peak calibration alpha source (Pu-239, Am-241, Cm-244) (National Nuclear Data Center, NuDat 2.6).

Source	Pu-239			Am-241			Cm-244	
Energy [keV]	5105.5	5144.3	5156.6	5388.0	5442.8	5485.6	5762.6	5804.8
Intensity [%]	11.94	17.11	70.77	1.66	13.1	84.8	23.1	76.9

container. The electronic chain consisted in a Cremat CR-110 charge-sensitive preamplifier module, an Ortec 572A shaping amplifier and a PicoScope 4424 digitizer controlled by a customized software developed in the LabVIEW environment. A voltage bias of 12 V was provided. The sketch of the experimental set-up is shown in Fig. 3.

2.4. Results

The pulse height spectrum acquired with the Hamamatsu S5972, reported in Fig. 4, shows that the main peaks associated to the alpha decay of Pu-239 (5.157 MeV), Am-241 (5.486 MeV) and Cm-244 (5.805 MeV) are properly identified. Moreover, three less intense peaks at 5.106 MeV, 5.443 MeV and 5.763 MeV are well distinguishable. Nevertheless, the spectrum is affected by other peaks originated by the contribution of scattered particles.

The pulse height spectrum measured with the Osram BPX65 photodiode indicates that the main alpha peaks of Pu-239, Am-241 and Cm-244 are clearly identified, as well as in the previous case. This spectrum, however, is less affected by the contribution of the scattered particles. Furthermore, the counting rate increases by about a factor 2, as expected, because of the greater effective area. For these reasons, the Osram BPX65 photodiode was finally selected. The measured energy resolution resulted to be about 25 keV FWHM.

The energy spectrum of the multi-peaks alpha source acquired with the Osram BPX65 photodiode was also compared with the spectrum measured by a EG&G ORTEC Silicon Charge Particle detector model BA-014-025-100 S, designed for high resolution charged particles spectroscopy and characterized by a sensitive area equal to 25 mm^2. Fig. 5 shows that the two distributions are in good agreement.

2.5. Assembly of the avalanche-confinement TEPC

The Osram BPX65 photodiode demonstrated to fulfil all the cited requirements: its very small size allows accommodating it inside the narrow cavity of the designed TEPC, its energy resolution is adequate and its cost is negligible. The external metal case TO-18 and the protecting glass lens were carefully removed to embed

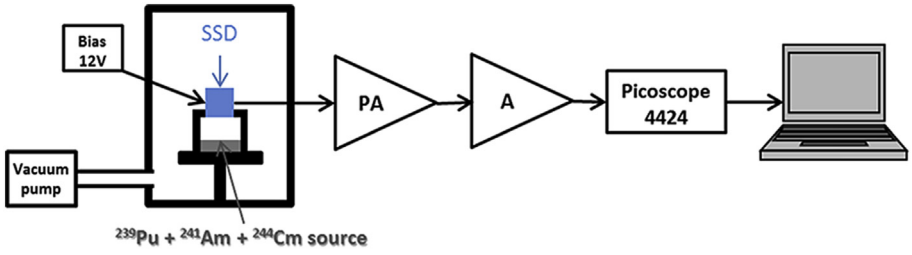

Fig. 3. Sketch of the experimental set-up for testing the response of the two selected photodiodes to alpha particles.

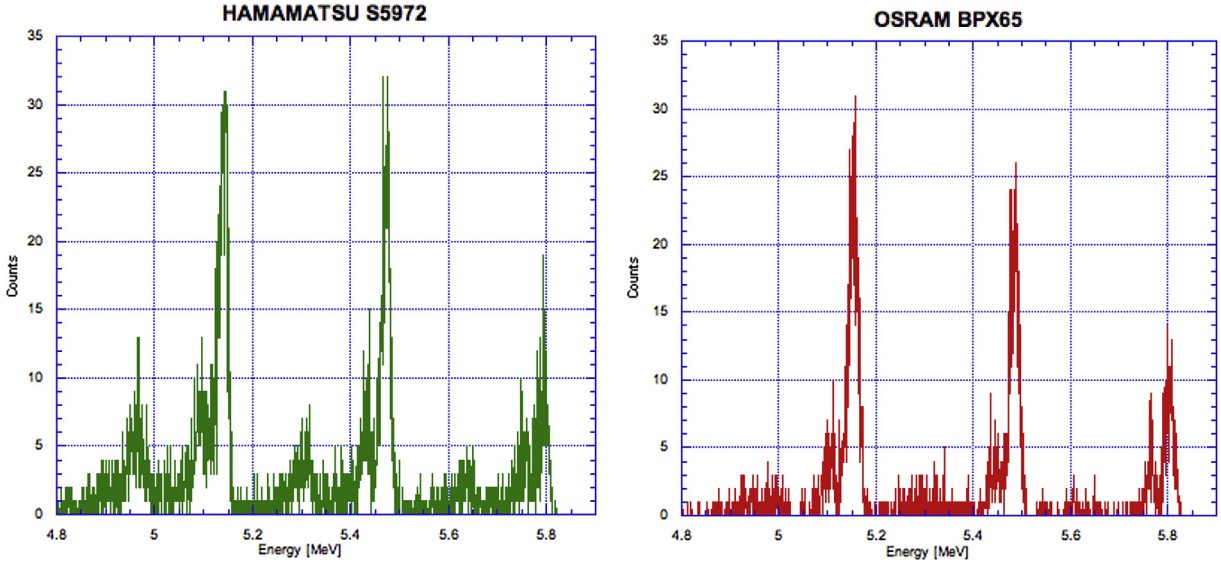

Fig. 4. Energy spectra of the multi-peak calibration alpha source (Pu-239, Am-241, Cm-244) acquired in vacuum conditions with the Hamamatsu S5972 photodiode (left) and with the Osram BPX65 photodiode (right).

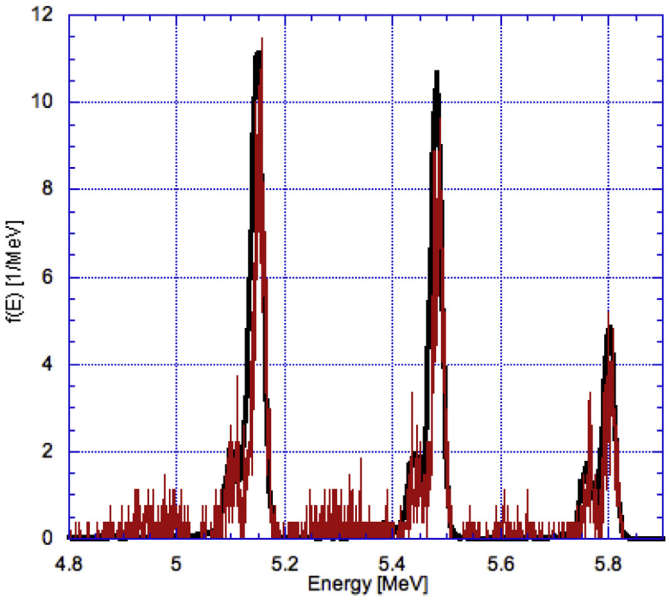

Fig. 5. Energy spectra of the multi-peak calibration alpha source (Pu-239, Am-241, Cm-244) acquired with the Osram BPX65 photodiode (red line) and with the reference EG&G ORTEC Silicon Charge Particle detector model BA-014-025100 S (black line). (For interpretation of the references to colour in this figure legend, the reader is referred to the web version of this article.)

the photodiode inside the available cavity of the TEPC.

A miniaturized Cm-244 alpha source was properly sealed, equipped with a mylar window and embedded in its reference position inside the TEPC aligned to the SSD (Fig. 6).

3. TEPC calibration method with the Cm-244 source and the Osram BPX65 photodiode

The single-event calibration method of the TEPC determines a conversion of the pulse height spectra h [mV] versus lineal energy y [keV·μm^{-1}]. If an internal alpha source is exploited, the energy calibration factor CF, which varies as a function of the simulated site size d_t and of the polarization of the electrodes ΔV, is defined with the following relation:

$$CF(d_t, \Delta V)\left[keV \cdot \mu m^{-1} \cdot mV^{-1}\right] = \frac{E_a(d_t)}{d_t \cdot V(d_t, \Delta V)}$$

where E_a is the amount of energy absorbed by tissue equivalent gas, which depends on the site size, due to alpha particles crossing the sensitive volume and V is the corresponding TEPC signal amplitude, which varies with both the simulated site size and the polarization of the electrodes.

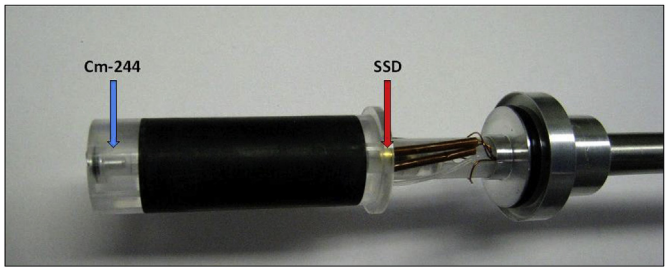

Fig. 6. The assembled avalanche-confinement TEPC (without the external protecting shell): the removable Cm-244 source and the selected SSD Osram BPX65 are indicated.

3.1. Measurement of the TEPC signal amplitude V

The block diagram of the electronic chain exploited for measuring the TEPC response to alpha particles in coincidence with the SSD signal by varying both the simulated site size and the polarization of the electrodes is shown in Fig. 7. It is composed by an Ortec 671 and a Silena 7611 shaping amplifiers for filtering signals from the SSD and the TEPC, respectively. The output signals from the amplifiers are connected to a PicoScope 4424-12 bit digitizer, which is controlled by a customized software developed in the LabVIEW environment. As already explained in the Introduction, only alpha particles crossing the TEPC sensitive volume parallelly to the anode wire are selected by the coincidence technique with the SSD signal, thus defining their path accurately.

The internal calibration method would require, ideally, a monoenergetic radiation source, since the amount of charge generated in the TEPC sensitive volume depends on the energy released by radiation. Nevertheless, the energy spectrum of the available Cm-244 source, reported in Fig. 8, shows the full energy peak at 5.18 MeV, instead of 5.805 MeV, and a broad distribution at lower energies, result of the self-absorption caused by the thickness of the source and the attenuation in mylar window.

For this reason, a proper threshold must be applied to the SSD signal in order to select the full energy peak only, by eliminating the distribution at lower energies. This is practically accomplished by the acquisition software, which allows collecting only TEPC signals due to alpha particles crossing the counter with direction parallel to the anode wire and having kinetic energy greater than a selectable value, chosen equal to 5 MeV. To give an example, Fig. 9 shows, on the left, the TEPC alpha spectra measured in coincidence with the SSD signal with and without a 5 MeV threshold in the alpha particles energy for a 170 nm simulated site with a potential difference at the electrodes equal to 400 V; the corresponding alpha spectra acquired with the SSD in the two different configurations are shown in the right side of Fig. 9. The acquisition performed without any energy threshold (green lines) results in a pulse height distribution of TEPC signals characterized by an asymmetric peak due to low energy alpha particles which deposit more energy in the gas. In fact, by selecting a 5 MeV threshold in the coincidence procedure (red lines), the TEPC alpha spectrum becomes more symmetrical and with no tail on the right.

To assess the calibration factor CF for each investigated operating condition (seven simulated site sizes d_t in the range 300 nm - 25 nm at different bias of the electrodes), the TEPC signal amplitude V is evaluated by calculating the centroid of the TEPC alpha spectrum measured in coincidence with the SSD signals above a value which corresponds to a 5 MeV threshold.

3.2. Calculation of the absorbed energy E_a

E_a is the amount of energy absorbed by the tissue-equivalent gas (which depends on the site size) due to alpha particles crossing the sensitive volume with direction parallel to the anode wire.

Nevertheless, when working at low gas pressures, the most energetic δ-rays emerging from the alpha particle track have ranges greater than the counter sensitive volume. Therefore, only a portion of the total released energy is actually collected and the energy carried away by these δ-rays must not be taken into account to perform lineal energy calibration (Colautti et al., 2000). Thus, the effective absorbed energy E_a is equal to the amount of energy released in the sensitive volume E_r by the alpha particle multiplied by an energy-dependent factor $f(E)$ which takes into account the percentage of energy lost.

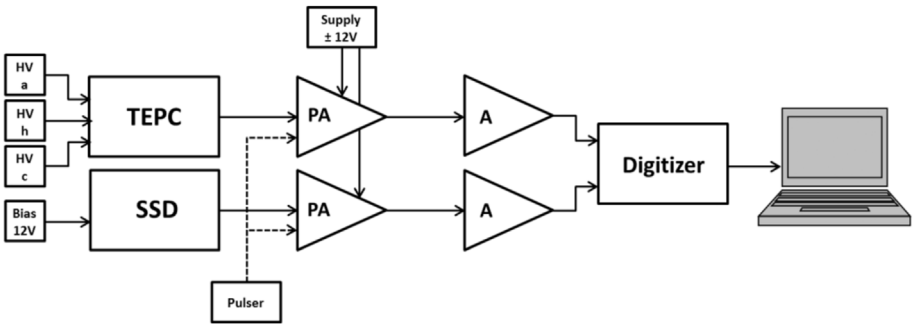

Fig. 7. Block diagram of the electronic chain for measuring the TEPC signal in coincidence with the SSD signal.

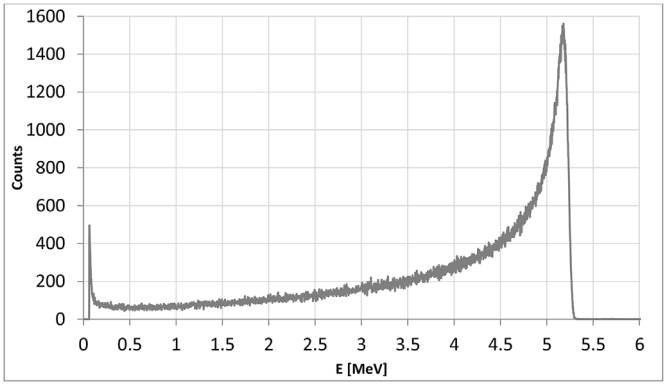

Fig. 8. Energy spectrum (in vacuum) of the thick Cm-244 alpha source embedded in the TEPC. This spectrum shows the full energy peak at 5.18 MeV, instead of 5.805 MeV, and a broad distribution at lower energies, result of the self-absorption caused by the thickness of the source and the attenuation in mylar window.

3.2.1. *The energy released in the sensitive volume E_r*

Since the energy released by alpha particles in all the investigated configurations is really small (about 28 keV and 2 keV at 300 nm and 25 nm, respectively), it is not possible to exploit the SSD to experimentally assess this value (the SSD energy resolution is about 25 keV FWHM). For this reason, the energy released in the sensitive volume of the TEPC is assessed with an algorithm which, by taking into account the Cm-244 alpha spectrum above 5 MeV (the same threshold set to measure the TEPC signal amplitude), calculates the energy lost by the alpha particle before entering the sensitive volume and inside the sensitive volume itself, by exploiting the range-energy tables available in literature (ICRU Report 49, 1993).

3.2.2. *Energy lost by delta rays*

The fraction *f(E)* of the energy released by primary particle which is actually absorbed by the gas is assessed by an algorithm based on the Chatterjee-Schaefer model (Chatterjee and Schaefer, 1976), which superimposes the counter sensitive volume to the alpha particle track structure and calculates the percentage of the energy lost. The theory of track structure distinguishes two regions: core and penumbra. The core is a narrow central zone with a radius in tissue far below 1 μm where the energy deposition mainly occurs via excitations and electron plasma oscillation, while the penumbra is a peripheral zone around the core where the energy deposition occurs mainly by ionization events due to energetic secondary electrons coming from the core. The extension of the penumbra region depends on the maximum energy transferred by primary particle to electrons, therefore by the speed of the primary particle. Because of their erratic trajectories, these secondary electrons can even re-enter into the core region losing energy through ionization events.

The theoretical analysis of track structure, described in details in

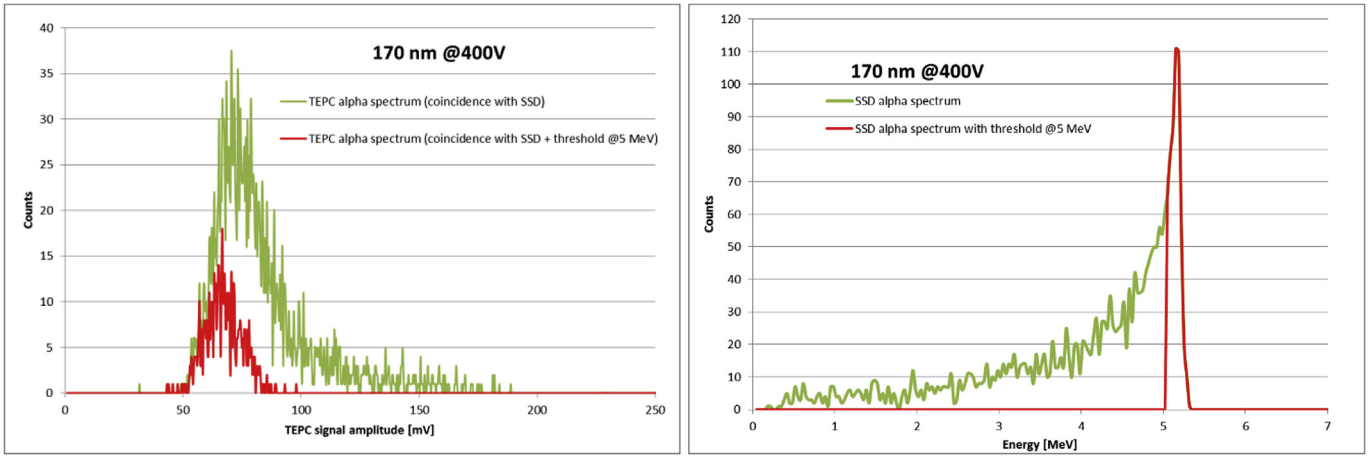

Fig. 9. TEPC alpha spectra measured in coincidence with the SSD signal with (red lines) and without (green line) a 5 MeV threshold in the alpha particles energy for a 170 nm simulated site with a potential difference at the electrodes equal to 400 V (on the left); corresponding alpha spectra acquired with the SSD in the two different configurations (on the right). (For interpretation of the references to colour in this figure legend, the reader is referred to the web version of this article.)

the cited reference, defines the following analytical expressions for the local energy densities $D_c(r)$ and $D_p(r)$ in the core and penumbra regions, as a function of the radial distance r from the center of the track:

$$D_C(r) = \frac{L_\infty}{2\pi R_C^2} + \frac{L_\infty}{4\pi R_C^2 ln\left(\sqrt{e}\ \frac{R_P}{R_C}\right)}$$

$$D_P(r) = \frac{L_\infty}{4\pi r^2 ln\left(\sqrt{e}\ \frac{R_P}{R_C}\right)}$$

where L_∞ is the unrestricted Linear Energy Transfer and e is the Euler's number.

In general terms, track structure can be described by an internal core characterized by a high energy density and a radial sub-micrometric extension, which is surrounded by a penumbra region where the energy density drops rapidly to very small values.

The fraction $f(E)$ of the energy actually absorbed by the gas is obtained by integrating the energy densities over the sensitive volume of the microdosimeter:

$$f(E) = \frac{1}{L_\infty}\left[\int_0^{R_C} D_C(r)2\pi r dr + \int_{R_C}^{R_P} D_P(r)2\pi r A(r)\, dr\right]$$

where $A(r)$ is the relative arc of a circumference centered in the particle track, given by the ratio between the circumference arc and the value of the circumference itself.

The radial extensions of both the core and the penumbra regions depend on energy of the primary particle. In our application, the energy of the alpha particle inside the sensitive volume must be known in order to evaluate $f(E)$. For simplicity, the energy of the alpha particle in the middle of the sensitive volume, is calculated by using the energy-range tables with the same procedure previously explained.

Table 3 lists the calculated values of E_r and $f(E)$ for all the studied configurations. As expected, both values diminish by decreasing the simulated site size due to the decrease in the number of gas molecules inside the sensitive volume.

The effective absorbed energy E_a is finally calculated by multiplying the amount of energy released E_r by alpha particles with the factor $f(E)$. As already explained, E_a depends on the simulated site size, i.e. on the gas pressure, but is not affected by the applied voltages to the electrodes. On the contrary, the TEPC signal amplitude V depends on both the simulated site size and the bias of the electrodes. For this reason, each calibration factor $CF(d_t,\Delta V)$ is referred to a specific simulated site and to a specific operating condition of the TEPC. This procedure is typically exploited for calibrating pulse height spectra of hadron and neutron beams, or mixed radiation fields. In the case of a pure photon field, a correction factor which takes into account the different number of generated electron-ion pairs must be applied (Bronić et al., 1988). It is defined as the ratio between the W-values for electrons and alpha particles, respectively.

Table 3
Calculated values of energy released E_r in the TEPC sensitive volume by alpha particles and fraction $f(E)$ of energy released which is actually absorbed for simulated site sizes d_t in the range 300–25 nm.

d_t [nm]	E_r [keV]	f(E)
300	27.8	0.91
170	15.8	0.87
100	9.4	0.82
50	4.8	0.76
35	3.4	0.73
30	2.8	0.72
25	2.4	0.70

4. Conclusions

The design of an innovative avalanche-confinement TEPC for microdosimetry at nanometric level accounted for a removable internal Cm-244 source and a very compact solid state detector inserted inside the sensitive zone for characterization and energy calibration. This set-up allows selecting only alpha particles crossing the TEPC sensitive volume parallelly to the anode wire by the coincidence technique with the SSD signal, thus defining their path accurately, and allows calibrating the TEPC by also varying the simulated site size and the polarization of the electrodes.

Since the available cavity for embedding the SSD detector is only 4.2 mm in diameter, a miniaturized detector was needed. Among different commercial photodiodes with small external cases, the Osram BPX65 photodiode was finally selected, with a measured energy resolution about 25 keV FWHM.

The proposed calibration method consists in the definition of a calibration factor which correlates the energy of the alpha particle which is absorbed in the gas and the corresponding TEPC signal amplitude as a function of the simulated site size and of the applied voltages to the electrodes. The effective absorbed energy is calculated with an algorithm which calculates the energy released in the sensitive volume and takes into account the energy lost by delta rays. Since the spectrum emitted by the internal Cm-244 source is not monoenergetic, because of self-absorption, the TEPC signal amplitude is evaluated by calculating the centroid of the TEPC alpha spectrum measured in coincidence with the SSD signals above a value which corresponds to a 5 MeV threshold.

Acknowledgements

This work was supported by the Italian National Institute for Nuclear Physics - INFN - Scientific Commission V in the framework of the MITRA (MIcrodosimetry and TRAck Structure) experiment.

References

Bronić, I.K., Srdoč, D., Obelić, B., 1988. The mean energy required to form an ion pair for low-energy photons and electrons in polyatomic gases. Radiat. Res. 115, 213–222.

Cesari, V., Colautti, P., Magrin, G., De Nardo, L., Baek, W.Y., Grosswendt, B., Alkaa, A., Khamphan, C., Ségur, P., Tornielli, G., 2002. Nanodosimetric measurements with an avalanche confinement TEPC. Radiat. Prot. Dosim. 99, 337–342.

Chatterjee, A., Schaefer, H.J., 1976. Microdosimetric structure of heavy ion tracks in tissue. Radiat. Environ. Biophys. 13, 215–227.

Colautti, P., Conte, V., De Nardo, L., Magrin, G., Alkaa, A., Ségur, P., Tornielli, G., Bordage, M.C., 2000. Code for Modelling Cylindrical TEPCs, in: Radiation Quality Assessment Based on Physical Radiation Interaction at Nanometer Level, pp. 82–90. LNL-INFN (REP) 161/2000, Legnaro.

De Nardo, L., Alkaa, A., Khamphan, C., Conte, V., Colautti, P., Ségur, P., Tornielli, G., 2002. A detector for track-nanodosimetry. Nucl. Instrum. Meth. A 484, 312–326.

Garty, G., Shchemelinin, S., Breskin, A., Chechik, R., Assaf, G., Orion, I., Bashkirov, V., Schulte, R., Grosswendt, B., 2002. The performance of a novel ion-counting nanodosimeter. Nucl. Instrum. Meth. A 492, 212–235.

Hamamatsu website.https://www.hamamatsu.com/jp/en/product/category/3100/4001/4103/S5972/index.html.

Hogeweg, B., 1973. Gas gain characteristics of a tissue-equivalent proportional counter, and their implications for measurements of event size distributions in small volumes. In: Proc. Fourth Symp. On Microdosimetry, vol. 5122, pp. 843–854.

International Commission on Radiation Units and Measurements (ICRU), 1993. Stopping Powers and Ranges for Protons and Alpha Particles. Report 49.

National Nuclear Data Center, NuDat 2.6. Brookhaven National Laboratory. http://

www.nndc.bnl.gov/nudat2/.
Osram website. http://www.osram-os.com/osram_os/en/products/product-catalog/infrared-emitters,-detectors-andsensors/silicon-photodetectors/photodiodes/pin-photodiodes-in-through-hole-package/bpx-65/index.jsp.
Pszona, S., Gajewski, R., 1994. An approach to experimental microdosimetry at the nanometer scale. Radiat. Prot. Dosim. 52, 427–430.
Schrewe, U.J., Brede, H.J., Pihet, P., Menzel, H.G., 1988. On the calibration of tissue-equivalent proportional counters with built-in alpha particle sources. Radiat. Prot. Dosim. 23, 249–252.
Wambersie, A., Hendry, J.H., Andreo, P., De Luca, P.M., Gahbauer, R., Menzel, H., Whitmore, G., 2006. The RBE issues in ion-beam therapy: conclusions of a joint IAEA/ICRU working group regarding quantities and units. Radiat. Prot. Dosim. 122, 463–470.